CARTESIAN GRID METHODS FOR FLOW IN IRREGULAR REGIONS

RANDALL J. LEVEQUE*

1. Introduction. Although a variety of powerful mesh generation techniques are now available to create body-fitting grids, the generation of a good grid for complicated, multi-element structures (e.g. full airplane configurations in 3D) is still a very time-consuming and manpower-intensive task. This has lead to a resurgence of interest in the possibility of using Cartesian grids for fluid dynamical calculations in regions with complicated geometry. There has been recent work in this direction both for the full potential equation (e.g. Wedan and South(1983), Ruppert et. al.(1986), Samant et. al.(1987)), and for the Euler equations, (Clarke et. al.(1986), Falle and Giddings(1988)).

This approach has several advantages:

- Mesh generation is straight forward and easily automated.
- On a uniform Cartesian grid, high resolution difference methods take a simple form and vectorize easily, leading to efficiencies of calculation.
- Grid refinement (needed to resolve nonsmooth regions of the boundaries as well as shocks and other flow features) is relatively simple, using for example the approach of Berger(1982) (see also Berger and Jameson(1985)).
- Grid effects that sometimes arise from nonuniformities in the mesh are also eliminated (although possible difficulties remain at grid refinement interfaces).

The primary difficulty with Cartesian grids is, of course, the boundary conditions. We wish to consider cell-centered finite volume methods for ease of guaranteeing conservation, but cells which are sliced off by the boundary may be orders of magnitude smaller than the regular cells away from the boundary. Figures 4a and 5a show typical situations in 2D. With standard explicit finite volume methods, the time step restriction is proportional to the area of the smallest cell. This follows from the CFL condition, since typically the fluxes determined at each cell interface affect only the two neighboring cells.

In this paper, I will describe a way to avoid this time step restriction by allowing information to propagate through more than one cell when necessary. Thus the CFL condition remains satisfied for larger time steps, and the time step can be chosen based on the regular Cartesian cells away from the boundary without restriction due to small cells at the boundary.

These boundary conditions are described here in 2D, but the same ideas would be applicable in 3D. The technique is briefly described in terms of wave propagation. More details may be found in (LeVeque 1987). These boundary conditions can also be rewritten to define fluxes at cell edges in cells near the boundary in such a way that the usual flux-differencing can still be applied to obtain updated cell values with the increased time step. This flux formulation has certain advantages. It allows the use of these boundary conditions together with any desired finite volume method (written in flux form) away from the boundary. Also, a joint project with Marsha Berger is currently under way to combine

[1] Mathematics Department, University of Washington, Seattle, WA 98195.

Supported in part by NSF Grants DMS-8601363 and DMS-8557319. To appear in the Proceedings of the Oxford Conference on Numerical Methods in Fluid Dynamics, March, 1988.

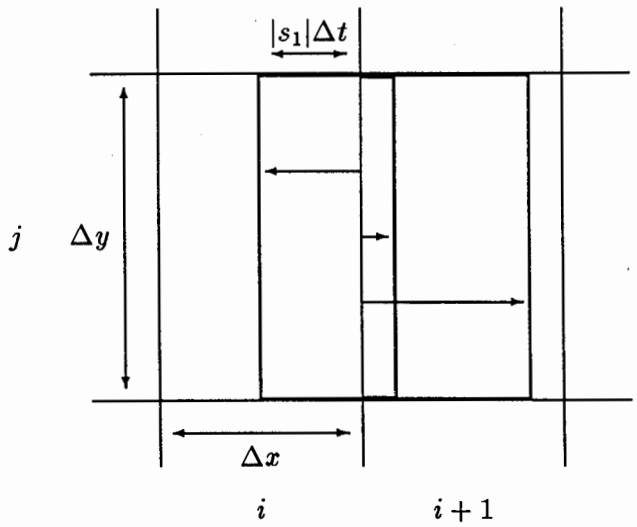

Fig. 1. *Portion of a 2D Cartesian grid with three waves propagating from the interface between cells* (i, j) *and* $(i+1, j)$.

these boundary conditions with her Cartesian mesh refinement code, which requires fluxes for interpolating from one grid to another. This flux formulation will be described in a future paper.

2. The wave propagation approach. The main idea of the wave propagation approach to defining a finite volume method is illustrated in Figure 1 for a regular Cartesian grid. Roe's approximate Riemann solver (Roe 1981) for the Euler equations is used to solve the Riemann problem in the x-direction between cells (i, j) and $(i+1, j)$. this gives a decomposition of $U_{i+1,j} - U_{ij}$ into three jumps, R_p $(p = 1, 2, 3)$,

$$U_{i+1,j} - U_{ij} = R_1 + R_2 + R_3 \tag{1}$$

propagating with speeds $dx/dt = s_p$, where

$$s_1 = \bar{u} - \bar{c}, \quad s_2 = \bar{u}, \quad s_3 = \bar{u} + \bar{c}. \tag{2}$$

Here $\bar{u}$ is an average fluid velocity and $\bar{c}$ an average sound speed. (There are actually four waves in the 2D Euler equations, but two of the waves always have the same speed $\bar{u}$ and can be combined.) These waves have the following effect on the neighboring grid cells:

For each wave:

$$\begin{aligned} &\text{if } s_p < 0 \text{ then} && U_{ij} \leftarrow U_{ij} - \frac{s_p \Delta t \Delta y}{\Delta x \Delta y} R_p \\ &\text{if } s_p > 0 \text{ then} && U_{i+1,j} \leftarrow U_{i+1,j} - \frac{s_p \Delta t \Delta y}{\Delta x \Delta y} R_p \end{aligned} \tag{3}$$

Note that the area swept out by the wave in time Δt is

$$A_{\text{wave}} = |s_p| \Delta t \Delta y$$

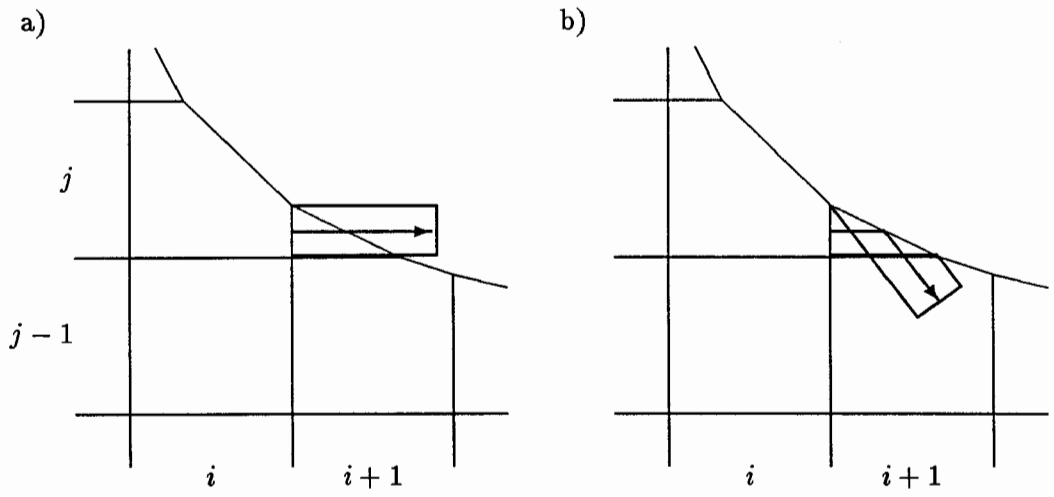

Fig. 2. *a) Wave propagating through a small boundary cell and out of computational domain. b) Reflected wave actually used.*

while the full cell area (for either cell (i,j) or $(i+1,j)$ is

$$A_{\text{cell}} = \Delta x \Delta y.$$

The appropriate value of U is thus updated by the ratio $A_{\text{wave}}/A_{\text{cell}}$ times the jump $\text{sgn}(s_p)R_p$ carried by the wave.

The cell values are updated by each wave from each neighboring Riemann problem in the x-direction and also by waves from Riemann problems solved in the y-direction in a similar manner (for example at the interface between cells (i,j) and $(i,j+1)$).

An obvious stability restriction for the method, as described in (3), is that $A_{\text{wave}}/A_{\text{cell}} \leq 1$. However, it is possible to ease this stability restriction by allowing waves that propagate a distance $|s_p|\Delta t > \Delta x$ to affect more than one neighboring cell. This is the idea behind the large time step generalization of Godunov's method described in one dimension in (LeVeque 1984, 1985).

In the work reported here the time step is restricted so that $|s_p|\Delta t < \Delta x$ (and $\Delta x = \Delta y$) and thus on the regular portion of the grid we have a standard finite volume method. By introducing piecewise linear approximations for the waves (with minmod slope limiters) this is converted into a high resolution (essentially second order accurate) method. See (LeVeque 1987) for details.

Near the boundary, however, the wave propagation viewpoint is used to deal with the small cells. Figure 2a shows a wave originating from the Riemann problem between cells (i,j) and $(i+1,j)$ that passes all the way through the small cell $(i+1,j)$. The portion of this wave that lies beyond the boundary is then reflected across the boundary and back into the computational domain, as shown in Figure 2b. The jump $\tilde{R}_p$ across this reflected wave is then used to update the values in each cell this wave overlaps, in this case $(i+1,j)$ and $(i+1,j-1)$. As before, the update made to U in each cell is $\tilde{R}_p$ multiplied by the

ratio of A_{wave} (the area of the cell intersected with the wave) divided by A_{cell} (the area of the cell). This ratio is always less than or equal to 1.

The jump $\tilde{R}_p$ across the reflected wave is equal to the jump across the incident wave R_p with the exception of the component of velocity normal to the boundary. This component of R_p is negated in $\tilde{R}_p$. This is the correct way to model the solid wall boundary condition and gives conservation (modulo our approximation of the boundary as piecewise linear).

In addition to waves coming from the cell interfaces, it is also necessary to solve a Riemann problem at the boundary face itself, in the direction normal to the boundary. This gives one additional wave propagating into the computational domain with speed $\bar{c}$, the local sound speed. The data for this Riemann problem consists of U from the interior boundary cell on one side, and $\tilde{U}$ on the other side, where $\tilde{U}$ equals U with the exception of the component of normal velocity, which is again negated. This wave is propagated normal from the boundary and affects neighboring cells in the same manner as described above for reflected waves.

In (LeVeque 1987) an additional wave splitting was also employed. Each wave R_p that arises from solving, for example, a Riemann problem in the x-direction can be further split into waves propagating oblique to the grid by solving a Riemann problem in the y-direction. In some situations this has stability advantages and may also give better resolution of 2D phenomena oblique to the Cartesian grid. However, in tests with stronger shocks (e.g. Mach 10) it has been found that this splitting can introduce some stability problems of its own. Moreover, it substantially increases the computational cost of the algorithm. More efficient splittings with better stability properties are currently being studied. In the calculations reported below, no secondary splitting has been used.

3. Numerical results. Figure 3 shows density contours for a Mach 4.62 shock wave advancing up a 40° ramp, with a double Mach reflection. This calculation was performed on an underlying 200×200 Cartesian grid, with the ramp cutting through the grid at a 40° angle. A section of the grid near the corner is shown in Figure 3a. The time step used gives a Courant number of about 0.5 relative to the regular cells (orders of magnitude larger relative to the smallest cells at the boundary). Ramp calculations of this nature are usually performed on a grid aligned with the ramp. For comparison purposes, one such calculation for this case may be found in Glaz, et. al. (1986).

Figure 4 shows a Mach 2.81 shock wave after hitting a circular cylinder. Again a 200×200 grid is used, a portion of which is shown in Figure 4a. For comparison see, for example, Yang and Lombard(1987), where the calculation is performed in polar coordinates.

As mentioned earlier, the method used here reduces to a very simple high resolution method on the regular portion of the grid. No attempt has been made yet to optimize this method. Techniques such a artificial compression of contact discontinuities have not been utilized. Some features are certainly smeared here, for example the slip lines within the double Mach reflection in the ramp calculation. Ultimately these boundary conditions will be used in conjunction with state-of-the-art finite volume methods on the regular portion of the grid and mesh refinement, which should yield superior results.

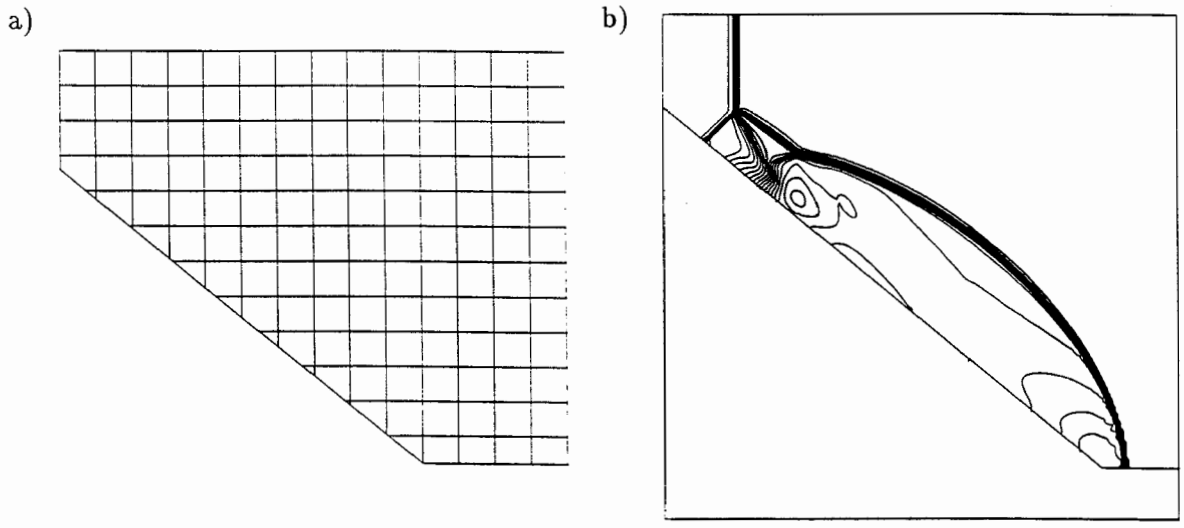

Fig. 3. *Mach 4.62 shock reflection from a 40° ramp. a) A portion of the Cartesian grid near the corner. b) Density contours of the computed solution.*

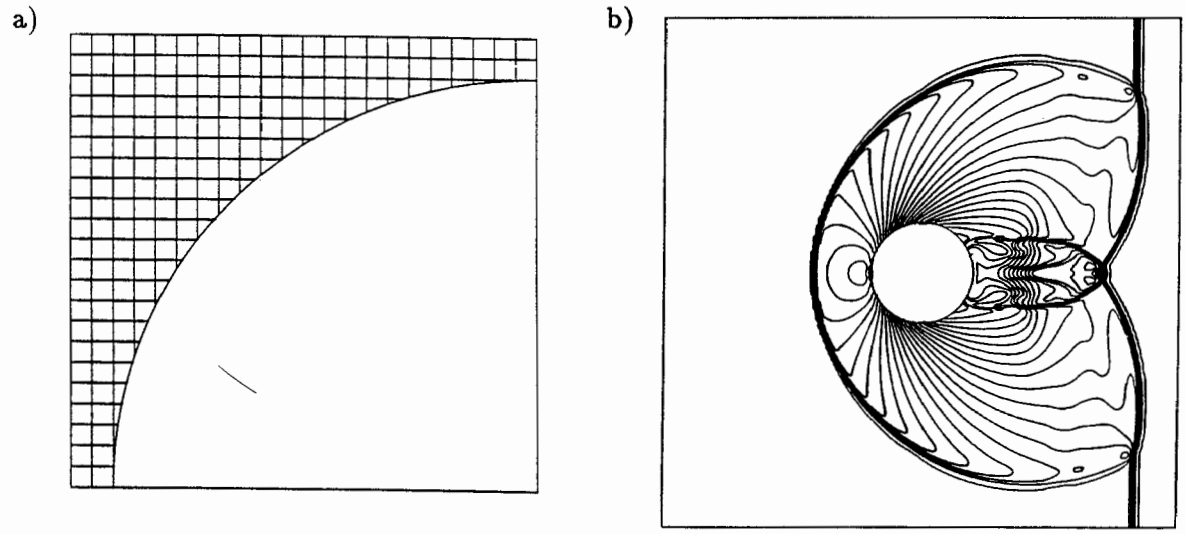

Fig. 4. *Mach 2.81 shock passing a cylinder. a) A portion of the Cartesian grid near the cylinder. b) Density contours of the computed solution.*

The main intent here is simply to demonstrate the feasibility of these boundary conditions for Cartesian grids in irregular regions. The accuracy obtained is comparable to what is produced by the same method in the absence of irregular boundaries (for example if the ramp is aligned with the grid). Most significantly, we obtain stable results using a time step based on the area of the regular grid cells.

REFERENCES

[1] Berger, M. (1982). Adaptive mesh refinement for hyperbolic partial differentail equations, Ph.D. dissertation, Computer Science Dept., Stanford University.

[2] Berger, M., and Jameson, A. (1985). Automatic adaptive grid refinement for the Euler equations, *AIAA J.* 23, 561-568.

[3] Clarke, D. K., Salas, M. D., and Hassan, H. A. (1986). Euler calculations for multielement airfoils using Cartesian grids, *AIAA J.* 24, 353-358.

[4] Falle, S. and Giddings, J. (1988). An adaptive multigrid applied to supersonic blunt body flow, These proceedings.

[5] Glaz, H. M., Colella, P., Glass, I. I., and Deschambault, R. L. (1986). A detailed numerical, graphical, and experimental study of oblique shock wave reflections, UTIAS Report No. 285, Univerisity of Toronto.

[6] LeVeque, R. J. (1984). Convergence of a large time step generalization of Godunov's method for conservation laws, *Comm. Pure Appl. Math.* 37, 463–477.

[7] LeVeque, R. J. (1985). A large time step generalization of Godunov's method for systems of conservation laws, *SIAM J. Num. Anal.*, 22, 1051–1073.

[8] LeVeque, R. J. (1987). High resolution finite volume methods on arbitrary grids via wave propagation, ICASE Report 87-68, to appear in *J. Comput. Phys.*

[9] Roe, P. L. (1981). Approximate Riemann solvers, parameter vectors, and difference schemes, *J. Comput. Phys.* 43, 357–372.

[10] Rubbert, P. E., Bussoletti, J. E., et. al. (1986). A new approach to the solution of boundary value problems involving complex configurations, in *Computational Mechanics — Advances and Trends*, AMD vol. 75, edited by A. K. Noor, 49-84.

[11] Samant, S. S., Bussoletti, J. E., et. al. (1987). TRANAIR: A computer code for transonic analysis of arbitrary configurations, AIAA Paper 87-0034.

[12] Wedan, B., and South, J. C. (1983). A method for solving the transonic full-potential equation for general configurations, AIAA Paper 83-1889.

[13] Yang, J. Y., and Lombard, C. K. (1987). Uniformly second order accurate ENO schemes for the Euler equations of gas dynamics, AIAA Paper 87-1166.